Since January 2020 Elsevier has created a COVID-19 resource centre with free information in English and Mandarin on the novel coronavirus COVID-19. The COVID-19 resource centre is hosted on Elsevier Connect, the company's public news and information website.

Biochemical and Biophysical Research Communications 476 (2016) 212–217

Contents lists available at ScienceDirect

Biochemical and Biophysical Research Communications

journal homepage: www.elsevier.com/locate/ybbrc

Enterovirus 71 induces anti-viral stress granule-like structures in RD cells

Yuanmei Zhu [1], Bei Wang [1], He Huang, Zhendong Zhao*

MOH Key Laboratory of Systems Biology of Pathogens, Institute of Pathogen Biology, Chinese Academy of Medical Sciences & Peking Union Medical College, Beijing, PR China

ARTICLE INFO

Article history:
Received 5 May 2016
Accepted 19 May 2016
Available online 20 May 2016

Keywords:
EV71
Stress granules
SG-like structures

ABSTRACT

Stress granules (SGs) are dynamic cytoplasmic granules formed in response to a variety of stresses, including viral infection. Several viruses can modulate the formation of SG with different effects, but the relationship between SG formation and EV71 infection is poorly understood. In this study, we report that EV71 inhibits canonical SGs formation in infected cells and induces the formation of novel RNA granules that were distinguished from canonical SGs in composition and morphology, which we termed 'SG like structures'. Our results also demonstrated that EV71 triggered formation of SG-like structures is dependent on PKR and eIF2α phosphorylation and requires ongoing cellular mRNA synthesis. Finally, we found that SG-like structures are antiviral RNA granules that promote cellular apoptosis and suppress EV71 propagation. Taken together, our findings explain the formation mechanism of SG-like structures induced by EV71 and shed light on virus-host interaction and molecular mechanism underlying EV71 pathogenesis.

1. Introduction

Enterovirus 71 (EV71), which belongs to the enterovirus genus of the *Picornaviridae* family, is known to cause hand, foot, and mouth disease (HFMD). In addition, acute EV71 infection can also lead to severe neurological manifestations and occasionally cause permanent paralysis or death. Currently, the pathogenic mechanisms underlying EV71 are unclear, so there are no effective antiviral treatments to control diseases caused by EV71. Therefore, further research is still needed to elucidate EV71 pathogenesis.

Formation of RNA granules is a prototypical stress response when cells suffering from viral invasion. Mammalian cells form two major kinds of cytoplasmic RNA granules to transiently store silenced messenger ribonucleoproteins (mRNPs), including stress granules (SGs) and processing bodies (PBs). SGs form in response to various environmental stresses and serve as a place for mRNA storage and triage. However, PBs are usually present in unstressed cells at modest levels and respond to stress with increased size and quantity [1]. There are two pathways that can induce SG formation, the most popular being phosphorylation of eIF2α by a family of serine/threonine kinases, including PKR, PERK, HRI and GCN2, and another being eIF2α-independent mechanisms such as cleavage of eIF4G scaffold protein or inhibition of eIF4E helicase [2]. Generally, canonical SGs contain translational silent mRNAs, 40S ribosomal subunits, eukaryotic initiation factors (e.g., eIF4G, eIF4A and eIF3), and RNA binding proteins (e.g., G3BP1, TIA1, TIAR, HuR and PABP) [3]. Among these components, RNA binding protein HuR, TIA1, and G3BP1 are usually considered key proteins and used as the markers of SGs.

Many studies have suggested that different viruses can modulate SG formation with different effects, and the virus-SG relationship may relate to viral pathogenicity. For example, respiratory syncytial virus and mouse hepatitis coronavirus induce stable SG formation during the course of infection to benefit viral propagation [4,5]. West Nile virus, Dengue virus and Rotavirus inhibit SG formation, presumably to antagonize their antiviral activity [6,7]. Poliovirus and CVB3 induce transient SG formation early during infection, then disassemble them to facilitate viral replication [8,9]. Vesicular stomatitis virus induces functional unknown cytoplasmic granules containing viral proteins and RNAs, but not some canonical SG markers [10]. Taken together, it can be concluded that, as the important constituent of host defense system, SGs play an important role in antiviral infection. EV71 was recently reported to induce SG formation in HeLa cells with high-dose, and viral protease $2A^{pro}$

* Corresponding author.
E-mail address: timjszzd@163.com (Z. Zhao).
[1] These authors contributed equally to this work.

http://dx.doi.org/10.1016/j.bbrc.2016.05.094
0006-291X/

was found to be responsible for the SG formation [11,12]. Despite these observations, the exact mechanism underlying EV71 induced SGs and the mutual regulative relationship between EV71 and SGs are still unclear.

Here, we report that EV71 infection induces novel 'SG-like structures' and inhibits canonical SGs formation. These SG-like structures are compositionally and morphologically different from canonical SG induced by arsenite or NDV. We also confirmed that the formation of SG-like structures induced by EV71 is dependent on PKR and eIF2α phosphorylation and requires ongoing cellular mRNA synthesis. Finally, we found that EV71 induced SG-like structures are antiviral RNA granules that promote cellular apoptosis and suppress EV71 propagation.

2. Materials and methods

2.1. Cells and viruses

Rhabdomyosarcoma (RD) cells and HeLa cells were purchased from ATCC. Cells were cultured in MEM or DMEM supplemented with 10% FBS and penicillin/streptomycin. EV71, which is a Fuyang strain (GenBank accession no. FJ439769.1), was propagated in RD cells. Newcastle disease virus (NDV) was kindly provided by Dr. Zhengfan Jiang (School of Life Sciences, Peking University, China) and propagated in HeLa cells.

2.2. Plasmids and siRNAs

shRNA sequences used in this study are as follows:

PKR: TACCAGTTTCAATGGTCATAA.
PERK: CCTCAAGCCATCCAACATATT.
TIA-1: GCCGTTGTTTACTTAAAGATTCTC.

HuR-siRNA (sc-35619) was purchased from Santa Cruz Biotechnology. Plasmid encoding mutant eIF2α(S52A) was cloned into the PcDNA3.1(+) vector.

2.3. Western blot, immunofluorescence

Western blot and immunofluorescence were carried out as previously described [13]. The antibodies and chemicals used in this study are listed in Supplementary Table 1.

2.4. Fluorescent in situ hybridization (FISH)

For mRNA-FISH, cells were fixed in 4% paraformaldehyde, permeabilized in 0.25% Triton X-100 and incubated overnight with biotinylated oligo (dT) probe in hybridization buffer at 43 °C. The next day, the cells were washed with 2 × SSC and incubated with streptavidin-Alexa Fluor FITC in 2 × SSC plus 0.1% Triton X-100 for 45 min. The cells were then washed with 4 × SSC and stained with 4,6-diamidino-2-phenylindole (DAPI) to detect nuclei. Images were captured with a laser confocal microscope (Leica) as described above.

2.5. Flow cytometry

Apoptotic cells were examined using an Annexin V-FITC/PI apoptosis assay kit (NEOBIOSCIENCE, FAK011) and a flow cytometer (BD CantoII) according to the manufacturer's instructions.

3. Results

3.1. EV71 induces granular structure formation in infected cells

Although numerous viruses have been reported to induce SG formation, the induced SGs are different in composition and time-effect. To investigate SG formation in EV71 infected cells, we categorized typical SG-defining markers and conducted a comprehensive time-course study examining their distribution. First, FISH was conducted to examine the distribution of poly(A)-mRNA, and the results showed that poly(A)-mRNA began to form cytoplasm foci at 6–7 h post-infection (pi) (Fig. 1A and Fig. S1). The distribution of the 40S ribosomal subunit was then investigated and ribosomal protein S11 were taken as its marker. The results revealed that S11 in EV71 infected cells stayed unchanged and no S11-positive foci emerged throughout the duration of infection (Fig. 1B and Fig. S1). Third, evaluation of initiation factor eIF4G and eIF3 showed they maintained an evenly distributed pattern and no cytoplasmic foci were formed over the whole period of infection (Fig. 1C and Fig. S1). Finally, several common RNA-binding proteins of SGs including G3BP1, PABP, TIA-1, TIAR and HuR were detected. Surprisingly, these RNA-binding proteins performed differently. Specifically, TIA1, TIAR and HuR were mainly detected within the nucleus in mock-infected cells, but EV71 infection induced their translocation to cytoplasm and formed noticeable granular structures. This change began at 5 h pi, peaked at 6–7 h pi, and was then attenuated. However, other RNA-binding proteins (G3BP1 and PABP) appeared to be static during the infection time, they remained dispersed in the cytoplasm and did not produce granules (Fig. 1D and Fig. S1). Taken together, these results suggested that EV71 infection can induce cytoplasmic foci containing some SG-defining markers. To further investigate the relationship of different protein aggregates in EV71 infected cells, multicolor fluorescent confocal monitoring of different markers was conducted to determine if these components were co-localized. We selected 7 h pi as the time-point since the foci formation of all molecules peaked at this time. The results showed that TIA1, TIAR, HuR and poly(A)-mRNA co-localized well with each other (Fig. 1E). To gain insight into whether these granular structures also contain EV71 viral components associated with viral replication, we examined the viral dsRNA, which are intermediates of viral RNA replication and viral RNA polymerase 3D required for viral RNA replication by indirect immunofluorescence. We noticed that the RNA granules contained a portion of the viral dsRNA, but not polymerase 3D (Fig. 1F), suggesting these structures may have some association with viral replication. Finally, to distinguish this structure from PBs, PB marker p54 was evaluated. The results showed that EV71 infection did not increase or enlarge p54 foci, but that it also destroyed the p54 foci originally present in mock-infected cells (Fig. 1G). These findings indicated that EV71 may play a disruption role in PB formation and ruled out the possibility that the observed RNA granules are PBs.

In summary, the above data indicate that EV71 can induce granular structures in infected cells, and that these structures contain a portion of typical SG markers including poly(A)-mRNA, TIA-1, TIAR, HuR and parts of viral dsRNA.

3.2. EV71 induces formation of novel SG-like structures and inhibits canonical SGs formation

The above results indicated that EV71 induced RNA granules are distinguished from canonical SG in composition and that some well-established SG markers are absent from these structures. To exclude the possibility that there were problems within our detection system, we used arsenite and Newcastle disease virus

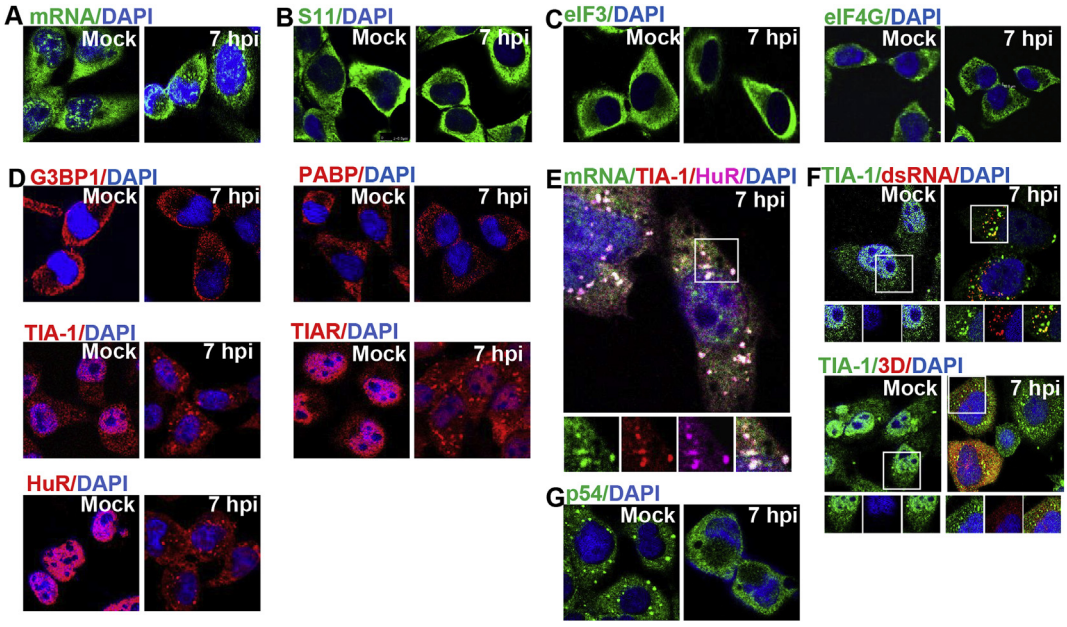

Fig. 1. EV71 induces granular structure formation in infected cells. **(A–D)** RD cells were mock-infected or infected with EV71 (MOI = 10) for 7 h, then stained for poly(A)-mRNA (A), ribosomal protein S11 (B), eIF3 and eIF4G (C), G3BP1, PABP, TIA-1, TIAR and HuR (D). **(E)** RD cells were infected with EV71 for 7 h and then co-stained for mRNA, TIA-1 and HuR. Insets show the magnified views of individual and merged channels of the boxed region. **(F, G)** RD cells were treated as described in (A), then co-stained for TIA-1, dsRNA or $3D^{pol}$ (F) or stained for p54 (G). Insets show the magnified views of individual and merged channels of the boxed region.

(NDV), which are well known to induce formation of typical SGs, and selected HuR and G3BP1 as the markers to monitor the canonical SGs formation. Consistent with previous studies, arsenite and NDV induced canonical SGs that contained G3BP1 and HuR that co-localized well (Fig. 2A). Moreover, these canonical SGs were morphologically different from EV71 induced RNA granules, being much larger in size (Fig. 2A). These findings suggested that EV71 induced RNA granules are not canonical SGs; therefore, we termed them 'SG-like structures'. To further explore the relationship between canonical SGs and EV71 induced SG-like structures, arsenite and NDV were used to induce SG formation in EV71 infected RD cells and SGs formation was assessed by double immuno-staining of G3BP1 and HuR. The results showed that the G3BP1 and HuR positive large particles induced by arsenite and NDV were no longer present and HuR positive microfoci were in their place (Fig. 2B and C) in EV71 infected cells. These findings indicate that EV71 infection inhibits canonical SGs formation and induces its own characteristic RNA granules.

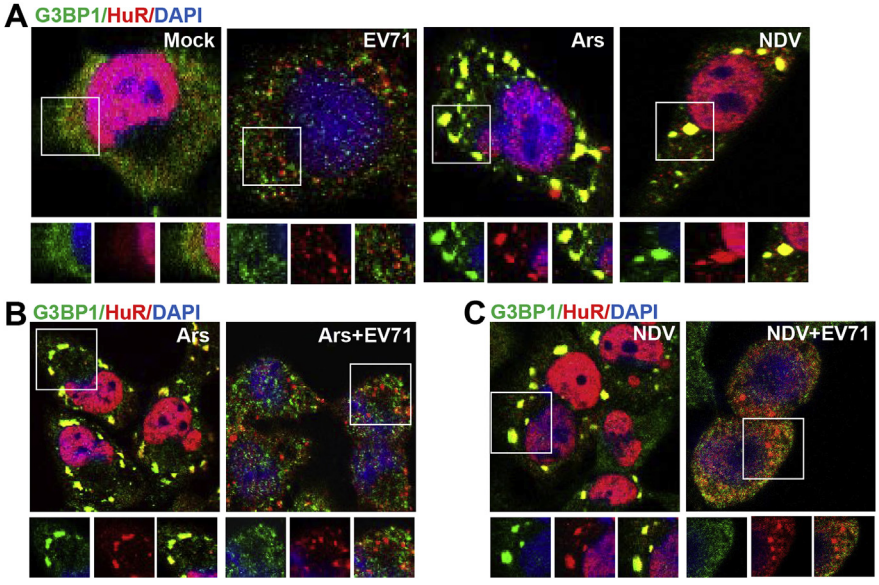

Fig. 2. EV71 inhibits canonical SGs formation and induced SG-like structures. **(A)** RD cells were mock-infected or infected with EV71 (MOI = 10), treated with 0.5 mM arsenite, infected with NDV, and then stained for G3BP1, HuR and nuclei. Insets show the magnified views of individual and merged channels of the boxed region. **(B)** RD cells were mock-infected or infected with EV71 for 7 h. Arsenite was added at 6.5 h post-infection, and cells were stained for G3BP1 and HuR. **(C)** NDV alone and NDV, EV71 (MOI = 1) co-infected cells were stained for G3BP1 and HuR. NDV were introduced into the experiment 3 h post-infection and it was continued for another 21 h. Insets show the magnified views of individual and merged channels of the boxed region.

3.3. Formation of EV71 induced SG-like structures is dependent on PKR and eIF2α phosphorylation and requires ongoing cellular mRNA synthesis

Phosphorylation of eIF2α is the major pathway leading to formation of SGs. To explore the potential mechanism by which EV71 induce and regulate the formation of SG-like structures, we first examined the kinetics of eIF2α kinases activation and phosphorylation of eIF2α. Among four eIF2α kinases, we selected PKR and PERK to evaluate since they are often associated with the stress of viral infection. Western blot analysis showed that phosphorylation of PKR, PERK and eIF2α displayed similar kinetics, beginning at ~6 h pi and then increasing as the infection proceeds (Fig. 3A). To discriminate the responsible kinase for eIF2α phosphorylation, we used corresponding shRNA to knock down the expression of PKR and PERK in RD cells, then infected these cells with EV71 and assessed the extent of eIF2α phosphorylation. The results showed that EV71 induced eIF2α phosphorylation was obviously decreased in PKR knock down cells relative to control-shRNA and PERK-shRNA treated cells (Fig. 3B), suggesting PKR is the dominant kinase to trigger eIF2a phosphorylation. Next, we checked the contribution of PKR to formation of EV71 induced SG-like structures using a RD cell line that stably expressed PKR-shRNA (PKR^{kd}) to monitor and quantify the SG-like structures after EV71 infection. The results showed that PKR down regulation severely decreased the frequency of SG-like structures in EV71 infected cells by about 50% per cell (Fig. 3C). The same results were also achieved using 2-AP, a PKR inhibitor (Fig. 3D). Finally, the role of eIF2α phosphorylation in SG-like structure formation was also determined. To accomplish this, we transfected RD cells with empty vector or phosphorylation-deficient mutant of eIF2α(S52A), then quantified the formation of SG-like structures under EV71 infection in both cells. We found that overexpression of phosphorylation-deficient eIF2α(S52A) obviously prevented the formation of SG-like structures, as indicated in a decrease in SG-like structures of about 30% relative to control cells (Fig. 3E). These findings suggest that EV71 induces SG-like structures formation through PKR-eIF2α phosphorylation.

Next, the contribution of each component to the process of SG-like structures formation was explored. We first checked the role of mRNA with ActD, which inhibits cellular mRNA synthesis but has no effect on EV71 RNA synthesis. The results showed that no SG-like structures were formed in mock infected cells, even though ActD caused obvious redistribution of HuR from the nucleus to the cytoplasm. However, in EV71 infected cells, ActD treatment significantly suppressed the formation of SG-like structures, suggesting that their formation is dependent on ongoing cellular mRNA synthesis (Fig. 3F). The roles of TIA-1 and HuR in this process were also checked by knock down of TIA-1, HuR or both. The results showed that neither of these are essential to the formation of SG-like structures (Fig. S2).

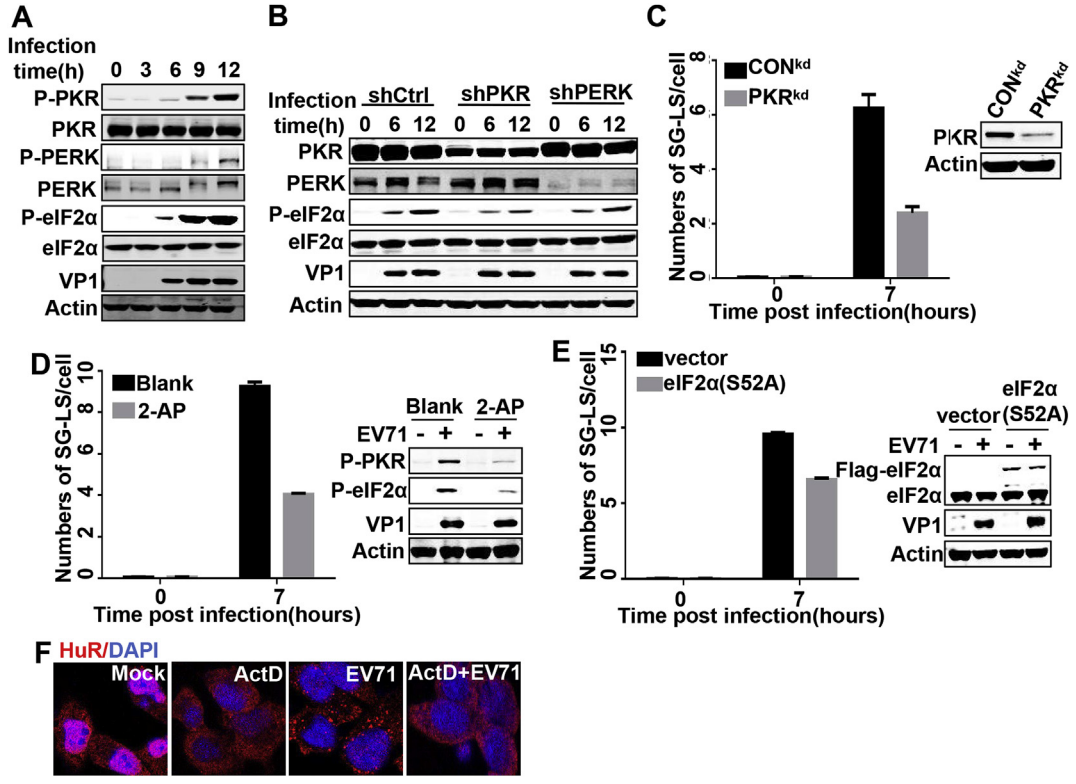

Fig. 3. SG-like structures formation in EV71 infected cells is dependent on PKR and requires ongoing cellular mRNA synthesis. **(A)** RD cells were mock-infected or infected with EV71 (MOI = 10) for the indicated time, the cells were then lysed and Western blot was performed with the indicated antibodies. **(B)** RD cells were transfected with corresponding shRNA for 48 h and then infected with EV71 for indicated time, after which Western blot was performed with the indicated antibodies. **(C)** The CON^{kd} and PKR^{kd} cells were mock-infected or infected with EV71 for 7 h, after which the induction of SG-like structures was quantified by counting the number of foci in each cell within three independent immunofluorescence images that each contained more than 20 cells. PKR knockdown efficiency was confirmed by Western blot. **(D)** Blank cells and cells treated with 6 mM 2-AP for 7 h were mock-infected or infected with EV71, after which formation of SG-like structures was quantified as described in (C) and cell lysates were subjected to Western blot with the indicated antibodies. **(E)** RD cells were transfected with empty vector or vector encoding eIF2α(S52A) for 36 h, then infected with EV71 for 7 h and formation of SG-like structures was quantified as described in (C) and cell lysates were subjected to Western blot with the indicated antibodies. **(F)** RD cells were mock-infected or infected with EV71 for 7 h and ActD was added at 3 h post-infection. The cells were then fixed and stained for HuR and nuclei.

3.4. SG-like structures are antiviral RNA granules that promote cellular apoptosis and suppress EV71 propagation

SGs have recently been demonstrated shown to play a regulatory role in cellular apoptosis [14]. To investigate the effects of SG-like structures on cellular apoptosis, we first took PKR as the target to block the formation of SG-like structures. We used PKR^{kd} cells and a PKR inhibitor, 2-AP, to achieve this goal, both of which have been shown to be available for attenuating SG-like structures formation (Fig. 3C and D). Western blot showed that cleavage of PARP, a marker of cellular apoptosis, was weaker in PKR^{kd} cells and 2-AP treated cells compared to that in control cells (Fig. 4A and B), indicating that SG-like structures may play a beneficial role in EV71 induced cellular apoptosis. The results shown in Fig. 4B were also verified by flow cytometry analysis with Annexin V-FITC/PI (Fig. 4C). Given that PKR is a multifunctional protein kinase in mammalian cells, we also evaluated downstream effectors of eIF2α to check the impact of SG-like structures on cellular apoptosis. To accomplish this, we transfected RD cells with empty vector or eIF2α(S52A). The results showed that cleavage of PARP was much weaker in eIF2α(S52A) transfected cells than that in the control (Fig. 4D), suggesting that inhibition of SG-like structures formation through eIF2α phosphorylation also negatively affected cellular apoptosis. Taken together, these results indicated that SG-like structures benefit cellular apoptosis in EV71 infected cells.

We next explored the impact of SG-like structures on EV71 propagation since both pro-and antiviral roles have been described for SGs. As shown in Fig. 3B, the viral protein VP1 accumulated equally in PKR knock down cells and control cells. However, the expression level of the viral protein did not completely reflect the viral propagation status, so viral particles released in cultural supernatants were further investigated. To accomplish this, RD cells were re-infected with cultural supernatants of different sources. Our results showed that RD cells re-infected with cultural supernatants form SG-like structure inhibited cells, including PKR knock down, 2-AP treatment or transfecting with eIF2α(S52A), expressed more VP1 protein than their corresponding control cells (Fig. 4E–G). We also titrated viral particles by TCID50 to further confirm the results and reached the same conclusion; namely, that the viral particles released in the cultural supernatants of PKR^{kd} cells had increased significantly (Fig. 4H). Overall, these results suggest that inhibition of SG-like structures formation positively affects EV71 propagation, indicating that EV71 induced SG-like structures are antiviral RNA granules.

4. Discussion

Eukaryotic cells initiate many responses when cells suffer from viral invasion, including formation of SGs [1]. It has been reported that PV and CVB3 induce canonical SG formation during the early stages of infection, after which viral 3C^{pro} cleaves the SG component G3BP1 to disassemble these structures [8,9]. CVB3, PV and EV71 are all members of the *Enterovirus* genus; however, they cause completely different types of diseases. According to previous studies, we selected mRNA, ribosomal protein S11, eukaryotic translation initiation factors (eIF3 and eIF4G) and RNA binding proteins G3BP1, PABP, TIA-1, TIAR and HuR as SG markers to examine whether EV71 can induce SG formation in this study. We found that EV71 infection induced formation of SG-like structures containing mRNA, TIA-1, TIAR, HuR and partial EV71 dsRNA, which are distinguished from canonical SG in morphology and composition, and that EV71 inhibited canonical SGs formation (Figs. 1 and

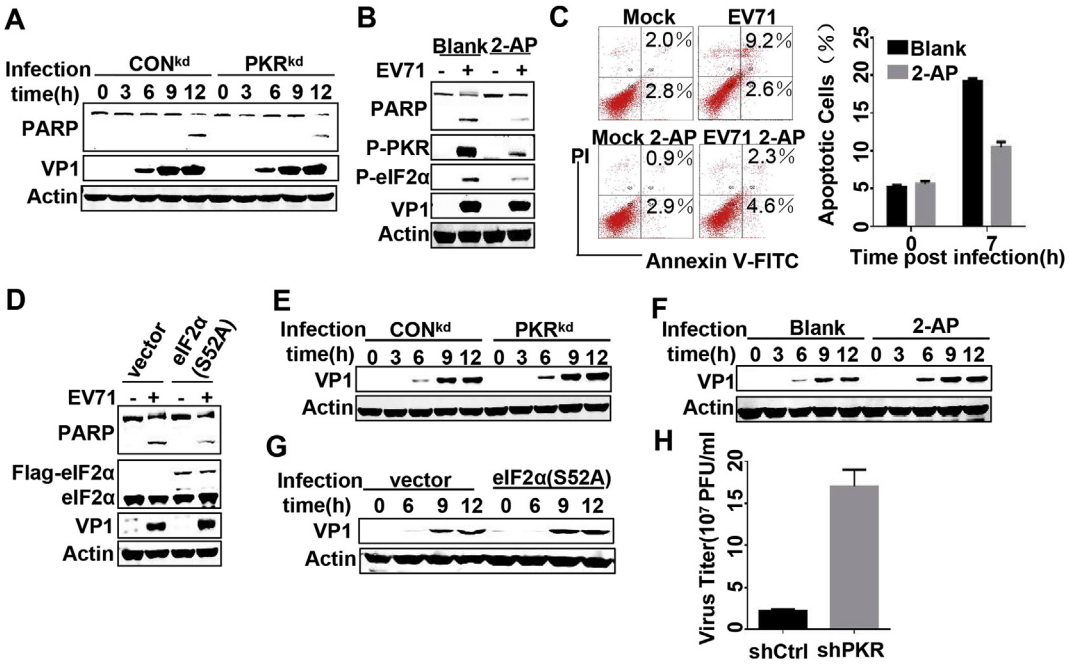

Fig. 4. SG-like structures promote cellular apoptosis and suppress EV71 propagation. **(A)** The Con^{kd} and PKR^{kd} cells were mock-infected or infected with EV71 for the indicated time, then lysed and subjected to Western blot with the indicated antibodies. **(B)** Blank cells and cells treated with 6 mM 2-AP for 12 h were mock-infected or infected with EV71, then lysed and subjected to Western blot with the indicated antibodies. **(C)** RD cells treated as described in (B) were stained with PI and Annexin V-FITC. The cells were analyzed on flow cytometry and the percentage of apoptotic cells was shown in the histogram. **(D)** RD cells were transfected with empty vector or vector encoding eIF2α(S52A) for 36 h, then infected with EV71, after which they were lysed and subjected to Western blot with the indicated antibodies. **(E)** The culture supernatants from EV71 infected CON^{kd} or PKR^{kd} cells were collected and RD cells were reinfected for the indicated time, after which the re-infected cells were lysed and Western blot was performed with indicated antibodies. **(F)** The culture supernatants from EV71 infected blank cells or cells treated with 6 mM 2-AP for 12 h were collected and the viral particle was detected as described in (E). **(G)** The culture supernatants from EV71 infected cells that had already been transfected with empty vector or eIF2α(S52A) were collected and the viral particles were detected as described in (E). **(H)** The CON^{kd} and PKR^{kd} cells were infected with EV71, after which the cultural supernatants were collected and viral particles were titrated by TCID50.

2). In this study, we also confirmed that G3BP1 was cleaved by EV71 protease 3C (data not shown), which is consistent with the situation of PV and CVB3 infection. Since G3BP1 is a critical SG component, we suspected that the cleaved G3BP1 may inhibit canonical SG formation in EV71 infected cells. In recent studies, Wu et al. reported that EV71 BrCr strain can induce canonical SGs formation in HeLa cells with a relatively high-dose EV71 (MOI = 50), and expression of EV71 $2A^{pro}$ alone was sufficient to cause SG formation [11,12]. In the present study, we also found EV71 $2A^{pro}$ alone can induce canonical SG formation (Fig. S3). However, this structure had not previously been detected in EV71 infected cells. We suspected that other viral components can antagonize the ability of $2A^{pro}$ to induce the canonical SG. For example, $3C^{pro}$ cleaves G3BP1 and may prevent EV71 from inducing canonical SGs; however, additional studies are needed to verify this. Additionally, the virus used in our study is a Fuyang stain, which caused the 2008 particular severe outbreak of HFMD in Fuyang, China. Differences in strains used among studies may also explain the conflicting findings in our study and others, and it is likely that SG-like structures formation in RD cells is EV71 strain specific.

It has previously been shown that SG formation can be induced by phosphorylation of eIF2α and interference with translation initiation factors (eIF4A, eIF4B, eIF4H or PABP) [2]. In our study, we demonstrated that EV71 induced RNA structure was also dependent on PKR-eIF2α phosphorylation, indicating that EV71 induced RNA granules are similar to SGs. Based on this similarity, partially shared components and a similar formation mechanism, we named these novel structures 'SG-like structures'.

In the present study, we found that SG-like structures promoted cellular apoptosis induced by EV71. This conclusion is in conflict with the features of classic SGs. Specifically, it has been reported that SGs can inhibit reactive oxygen species (ROS)-dependent apoptosis by suppressing the elevation of ROS, and this function of SGs is executed by G3BP1 and USP10 [14]. The absence of G3BP1 in EV71 induced SG-like structures may explain why this RNA structure does not have anti-apoptosis properties. However, additional in-depth studies are needed to investigate the mechanisms by which SG-like structures promote apoptosis.

In this study, we also found that EV71 induced SG-like structures are antiviral RNA granules. When SG-like structures were inhibited, the viral particles released into the cultural supernatants increased significantly. However, the expression of viral protein VP1 in cells did not exhibit obvious differences, suggesting that SG-like structures may not affect initiation of EV71 RNA replication and viral protein synthesis, but that they affect other steps of viral propagation such as viral particle assembly or release.

RNA binding proteins such as TIA-1 and G3BP1 are considered key constituents of canonical SGs since they play crucial roles in mediation of SG formation via their self-aggregation ability. Overexpression of these molecules results in SG formation, while their downregulation prevents the cells from forming SGs. To determine the key components in EV71 induced SG-like structures, we investigated each component of these structures. Among the identified constituents, only ongoing cellular mRNA synthesis is required for its formation, while TIA-1 and HuR did not influence the formation of these structures. We speculate that other critical molecules may exist in these structures, which would compensate for or substitute the function of TIA-1 and HuR; thus, more detailed studies are needed to elucidate the complicated composition of this structure.

In summary, our study demonstrated that EV71 infection could induce its own SG-like structures that differ from canonical SG in morphology and composition, and that EV71 suppresses canonical SG formation. The formation of SG-like structures is dependent on phosphorylation of PKR and eIF2α and requires ongoing cellular mRNA synthesis. We also found that SG-like structures promote cellular apoptosis and inhibit EV71 viral propagation. Our findings improve our understanding of the virus-host interaction and provide new insights into the pathogenic mechanism underlying EV71infection.

Conflict of interest

None.

Acknowledgments

We thank Dr. Zhengfan Jiang for providing NDV-GFP virus (School of Life Sciences, Peking University, China). This work was supported by National Natural Science Foundation of China (NSFC 31400159 and NSFC 81572008) and Innovative Research Team in University (IRT13007).

Appendix A. Supplementary data

Supplementary data related to this article can be found at http://dx.doi.org/10.1016/j.bbrc.2016.05.094.

References

[1] J.P. White, R.E. Lloyd, Regulation of stress granules in virus systems, Trends Microbiol. 20 (2012) 175–183.
[2] R.E. Lloyd, How do viruses interact with stress-associated RNA granules? PLoS Pathog. 8 (2012) e1002741.
[3] J.R. Buchan, R. Parker, Eukaryotic stress granules: the ins and outs of translation, Mol. Cell 36 (2009) 932–941.
[4] M.E. Lindquist, A.W. Lifland, T.J. Utley, et al., Respiratory syncytial virus induces host RNA stress granules to facilitate viral replication, J. Virol. 84 (2010) 12274–12284.
[5] M. Raaben, K.M. Groot, P.J. Rottier, et al., Mouse hepatitis coronavirus replication induces host translational shutoff and mRNA decay, with concomitant formation of stress granules and processing bodies, Cell Microbiol. 9 (2007) 2218–2229.
[6] M.M. Emara, M.A. Brinton, Interaction of TIA-1/TIAR with West Nile and dengue virus products in infected cells interferes with stress granule formation and processing body assembly, Proc. Natl. Acad. Sci. U. S. A. 104 (2007) 9041–9046.
[7] H. Montero, M. Rojas, C.F. Arias, et al., Rotavirus infection induces the phosphorylation of eIF2alpha but prevents the formation of stress granules, J. Virol. 82 (2008) 1496–1504.
[8] J.P. White, R.E. Lloyd, Poliovirus unlinks TIA1 aggregation and mRNA stress granule formation, J. Virol. 85 (2011) 12442–12454.
[9] G. Fung, C.S. Ng, J. Zhang, et al., Production of a dominant-negative fragment due to G3BP1 cleavage contributes to the disruption of mitochondria-associated protective stress granules during CVB3 infection, PLoS One 8 (2013) e79546.
[10] P.X. Dinh, L.K. Beura, P.B. Das, et al., Induction of stress granule-like structures in vesicular stomatitis virus-infected cells, J. Virol. 87 (2012) 372–383.
[11] S. Wu, L. Lin, W. Zhao, et al., AUF1 is recruited to the stress granules induced by coxsackievirus B3, Virus Res. 192 (2014) 52–61.
[12] S. Wu, Y. Wang, L. Lin, et al., Protease 2A induces stress granule formation during coxsackievirus B3 and enterovirus 71 infections, Virol. J. 11 (2014) 192.
[13] B. Wang, X. Xi, X. Lei, et al., Enterovirus 71 protease 2Apro targets MAVS to inhibit anti-viral type I interferon responses, PLoS Pathog. 9 (2013) e1003231.
[14] M. Takahashi, M. Higuchi, H. Matsuki, et al., Stress granules inhibit apoptosis by reducing reactive oxygen species production, Mol. Cell Biol. 33 (2013) 815–829.